Noise Reduction for Efficient In-Vehicle Respiration Monitoring with Accelerometers

Joana M Warnecke, Ju Wang and Thomas M Deserno
Peter L. Reichertz Institute for Medical Informatics of TU Braunschweig and Hannover Medical School, Braunschweig, Germany

***Abstract*—Toward ubiquitous vital sign monitoring, de-noising is still challenging under real driving conditions. This work intends to investigate the performance of de-noising with an additional accelerometer in different positions for respiratory rate (RR) estimation. One accelerometer was attached to the seatbelt to record the signal of respiratory movements. For noise recording, two accelerometers were attached to the car seat in two ways, i.e., (1) on the front and back side (F-B) of the seat and (2) on the left and right side (L-R). The recorded noise information was used to suppress noise in the signal and in the frequency domain. The experiment was conducted under three driving conditions, i.e., *engine on*, *flat road* and *uneven road*. The median of the estimated RR is for F-B 2.15 breaths per minute (bpm), and for L-R 0.93 bpm. The medians for the three driving conditions are 0.81 bpm (*engine on*), 0.86 bpm (*flat road*), and 2.53 bpm (*uneven road*) respectively. In conclusion, suitable positions for the noise accelerometer are on the left and right side of the seat. Further approaches are in demand to achieve a more stable estimation for the most dynamic driving conditions such as uneven roads.**

I. Introduction

Technological progress is continuously improving the possibilities of healthcare [1,2,3]. However, many existing potentials of improvement are still far from being fully exploited. In particular, the environments in which we spend plenty of time, such as home, work and the car are appropriate for the monitoring of vital signs. This monitoring enables earlier detection of diseases because it allows conclusions about a person's health [4].

Especially people who frequently use the car for commuting, spend a considerable amount of time in their car. Nowadays, the type of driving is facing a paradigm shift to autonomous driving [5], which makes it possible to use driving time in a different way, e.g., for a medical check-up. The recording of vital signs and the monitoring of health could transform a car into a diagnostic space. So far, it is not established to record vital signs in cars, which is due to ethical but also to technical difficulties. Another problem is the low signal-noise-ratio under real driving conditions [6,7]. Due to the low signal-noise-ratio, the processing of the vital signs during driving is an unsolved problem.

Respiration monitoring yields the health state of a person. The RR can be detected by a three-axis accelerometer, which records the respiration movements and is confirmed by other researches [8,9]. The best position for measuring respiration on the seatbelt with an accelerometer was determined in a previous experiment and is the side-waist position [10]. But under real driving conditions, the recorded signal is noisy. For this reason, the signal processing methods applied to reduce noise.

This work used additional accelerometers for noise suppression, which is also widely used for audio signals [11]. We intend to answer whether using additional accelerometers is a suitable method for reducing noise towards estimating the RR and which positions are appropriate for the additional accelerometers during autonomous driving.

II. Methods

A. Data Acquisition

A measurement system was built up in a test car (Mini One, 66 kW, BMW, Munich, Germany). Because the passenger in a non-autonomous vehicle does not perform any driving activities, we chose a passenger seat to place the sensors for the simulation of autonomous driving. Three Shimmer3 (Shimmer, Ireland) sensor modules including two inertial measurement units (IMU) and one electrocardiogram (ECG) unit were deployed to the passenger car seat system for data collection. The IMU is embedded with tri-axial accelerometers. Besides of tri-axial accelerometers, the ECG unit is embedded with the ECG module, which can generate ECG-derived respiratory signal.

Based on our previous experiment, the position of side-waist is appropriate to reflect the respiratory movements [10]. Therefore, the ECG unit was attached to the seatbelt at the position side-waist to monitor respiratory movements using the embedded accelerometer. Meanwhile, the electrodes were attached to tester's skin for collecting the ECG-derived respiratory signal. The ECG unit was named *Sensor 1*. To record noise generated by the car, two IMU, namely *Sensor 2* and *Sensor 3*, were attached to preselected positions around the seat in two ways:

(1) F-B: attaching the two sensors to the front side and back side of the seat (Fig. 1 a);

(2) L-R: attaching the two sensors on the left side and right side of the car seat (Fig. 1 b).

The sampling rates for all sensors were configured as 204.8 Hz. A laptop (Latitude 5480, Dell, Texas, USA) was carried in the car for monitoring data in real-time and collecting data in a database. The *Sensor 1* was connected to a laptop via Bluetooth, and its data were directly transferred to the database. During the experiments, the data generated by *Sensor 2* and *Sensor 3* were stored in the embedded SD cards and manually transferred to the database afterward.

978-1-5386-1311-5/19/$31.00 ©2019 IEEE

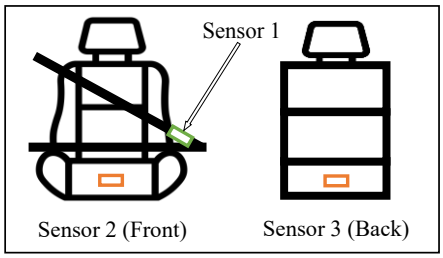

(a)

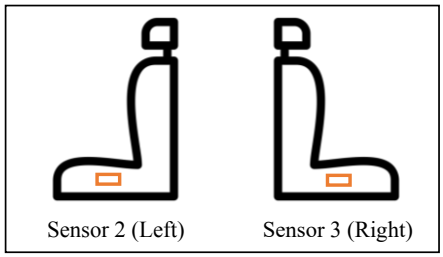

(b)

Figure 1. Two ways (F-B and L-R) of the placements of two IMU (*Sensor 2* and *Sensor 3*) at the passenger seat.

B. Data Processing

Sensor 1 was used to generate acceleration, which records the respiration signal and noise and ECG-derived respiratory signal as reference RRs. *Sensor 2* and *Sensor 3* were used to generate acceleration and records only noise. A preprocessing pipeline was applied to all acceleration data generated in each session (Fig. 2).

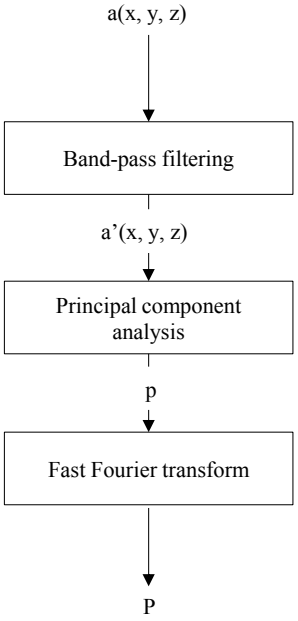

Figure 2. Accelerometer sensor data processing flowchart.

Firstly, a Butterworth band-pass filter was applied to tri-axial acceleration, a(x, y, z), and the cutoffs were set to [0.05 Hz, 1 Hz] according to healthy people's normal RRs. Afterward, the principal component analysis (PCA) method was leveraged to the filtered tri-axial acceleration, a'(x, y, z) and the first principal component p, was considered the fusion of the tri-axial acceleration into a one-dimension.

Finally, the temporal data was transformed into frequency domain P, using fast Fourier transform (FFT). The sequences within the frequency interval [0.05 Hz, 1 Hz] were selected.

Here we used P_1, P_2 and P_3 denote the selected FFT sequences of acceleration data generated by *Sensor 1*, *Sensor 2*, and *Sensor 3* respectively. The magnitudes of P_1 represent the frequency distribution of the mixture of signal and noise, whereas the magnitudes of P_2 and P_3 can only reflect the frequency distribution of the noise.

A frequency component with a higher magnitude in P_2 or P_3 implies higher noise at the frequency. We defined a function (Equ. 1) to calculate the suppression factor (SF) that was used to suppress the frequency components in P_1 according to the magnitudes of P_2 and P_3. The kth SF for P_1 can be calculated by,

$$\mathrm{SF}(k) = \mathrm{e}^{-\frac{\mathrm{a}|\mathrm{P}_2(k)|+(1-\mathrm{a})|\mathrm{P}_3(k)|}{\mu(|\mathrm{P}_1|)}} \quad (1)$$

where $|\mathrm{P}_2(k)|$ and $|\mathrm{P}_3(k)|$ denote the kth amplitude in FFT series referring to the IMU, i.e., *Sensor 2* and *Sensor 3* respectively, a and b are the weights assigned to the two sensor data, and $\mu(|\mathrm{P}_1|)$ denotes the mean value of the amplitudes of the P_1. In this work, a = 0.5. The frequency distribution of nothe ise-suppressed (ns) signal was calculated by

$$\mathrm{P}_{\mathrm{ns}}(k) = \mathrm{SF}(k)\cdot\mathrm{P}_1(k) \quad (2)$$

The highest peak in the frequency interval [0.05 Hz, 1 Hz] is used to derive the corresponding respiratory frequency f_r, and estimate the RR, RR_E using $f_r \cdot 60$ s.

C. Experimental Design

We considered three normal driving conditions, i.e.,

- *Engine on*: start the engine and keep the car parking.
- *Flat road*: drive the car on a flat road without potholes with a speed of 20 – 30 km/h.
- *Uneven road*: drive the car on a gravel parking lot with a speed 10 ± 2 km/h.

Three healthy volunteers participated in the experiment as testers. The BMI and gender of the testers T1, T2 and T3 were 20.8, 22.0, 23.4 and male, female and male respective. During the entire experiment, all testers were guided to sit in a state of relaxation on the passenger seat. The test car was driven under the three above-mentioned conditions. The duration for each driving condition was two to three minutes, namely a *session*. Each tester experienced two sessions under a certain condition. We conducted a two-round experiment for each condition. On the first round, the two IMU were attached to the left-right position (Fig. 1 b); and on the second round, the two IMU were attached to the front-back position (Fig. 1 a). Therefore, we collected a total of 36 sessions data.

D. Results Analysis

We apply impedance pneumography to detect respiration by measuring the impedance across the tester's chest using adhesive ECG electrodes. The impedance changes with inhalation and exhalation. For the ECG measurement, we placed four reference electrodes for the bipolar limb leads (RA, LA, RL, and LL). To get the ground truth of RR, the ECG-derived respiratory movement signal was visualized, and

we manually counted the waves of the breathing movement by three separate persons. We calculated the difference between the estimated RRs and the reference RRs. To compare the results, these differences were displayed with the widely used Bland-Altman plot [12]. To evaluate the performance of the proposed methods for different driving conditions, the results for the three conditions were compared. In order to investigate the difference in placing IMU, the results for the various ways of placements were also compared.

III. Results

A. *Raw Data of Accelerometer and Filtered Data*

The band-pass filter can easily remove high-frequency noise. When the sensors were attached to the seat, the orientation was not taken into account. The respiratory movements can be reflected by multiple axes of the acceleration (Fig. 3: *Sensor 1*). Apparently, the two IMU demonstrate different signals due to their placements (Fig. 3: *Sensor 2 (Front)* and *Sensor 3 (Back)*).

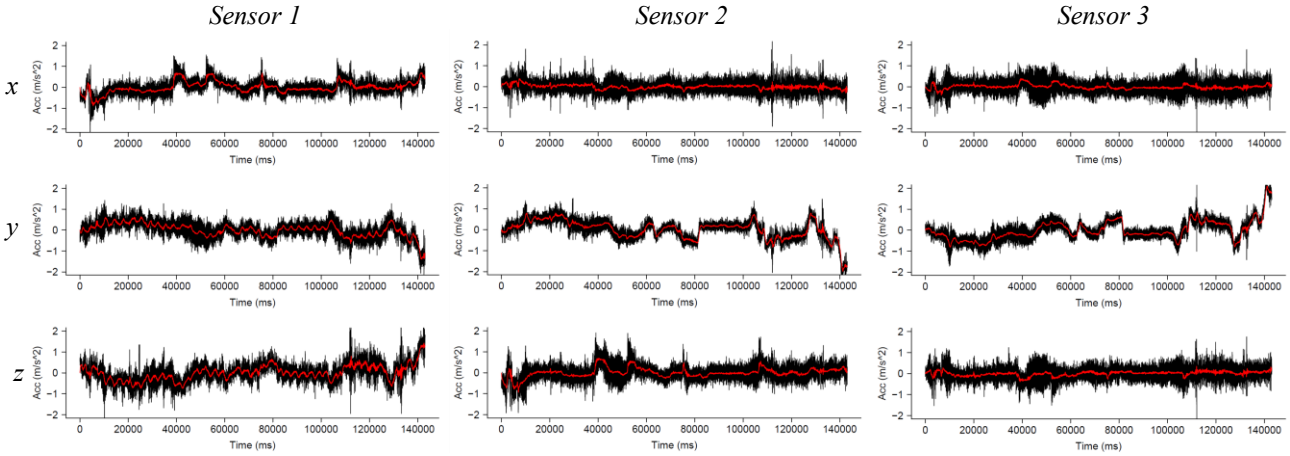

Figure 3. Raw data (black) and filtered data (red) of *Sensor 1*, *Sensor 2*, and *Sensor 3*.

B. *One-Axis Signal using PCA*

The PCA simplified data processing. Regardless of the orientation of the sensors, all three channels (axes) signals were combined into one axis. When the signal showing in Fig. 3 were processed by PCA, we obtained three one-dimension signals for the three sensors (Fig. 4). Similarly, as the raw data, the PCA signals of *Sensor 2* and *Sensor 3* showed the data in the opposite. The PCA of *Sensor 1* can demonstrate the waveforms of respiratory movements and the entire curve was distorted by noise.

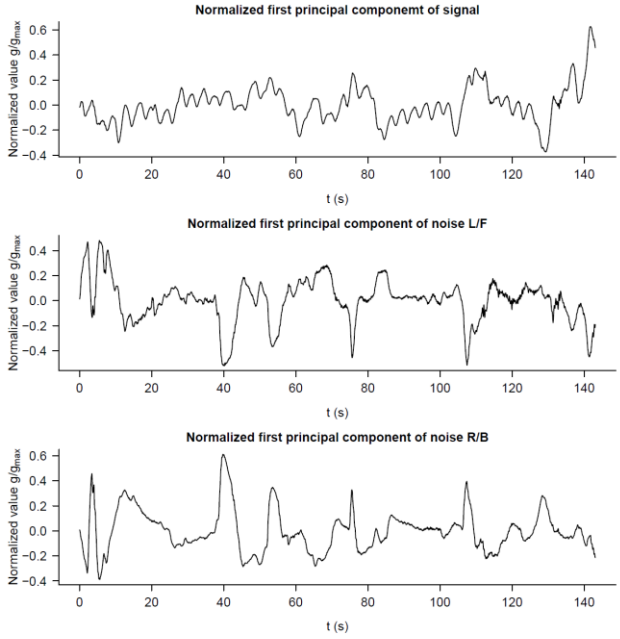

Figure 4. The first principal components of the three sensors.

C. *Information Exhibited in the Frequency Domain*

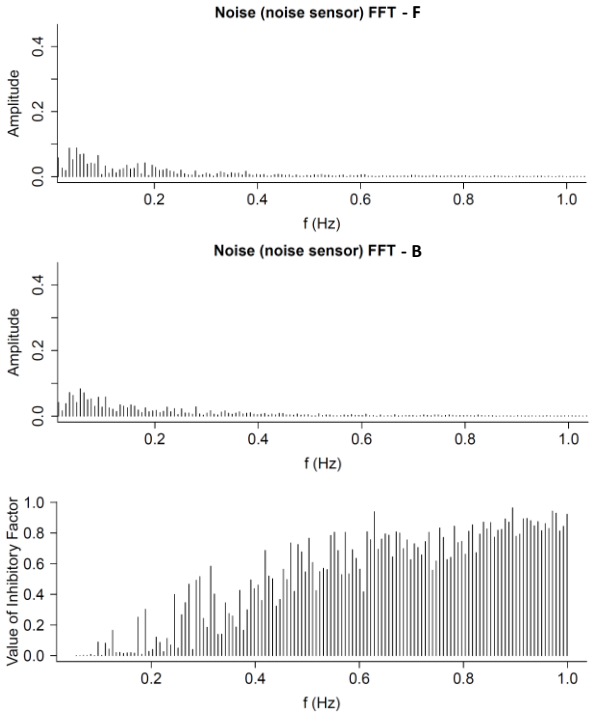

Figure 5. FFT of two noise sensors (the upper two bar charts) and the SF calculated based on them (the bottom bar chart).

The nature of equation (1) implies that higher noise distribution in a certain frequency implies more suppression on that frequency component (Fig. 5). The real respiratory signal can be highlighted by applying the SF to the FFT of *Sensor 1* data (Fig. 6).

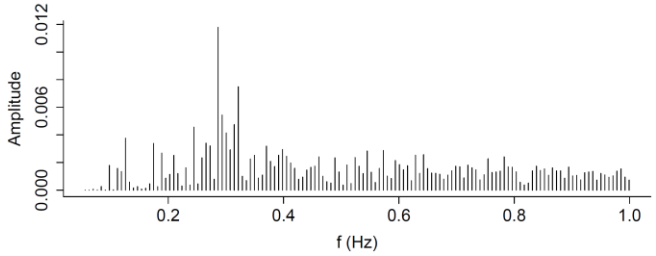

Figure 6. Frequency distribution of noise suppressed data from *Sensor 1*.

D. Comparison Between Reference RR and Estimated RR

The comparison shows that the mean value of the difference between the estimated RR and reference RR is 3.04 bpm. Nevertheless, there are three outliers where the difference between estimated RR and reference RR exceeds 10 bpm (Fig. 7). These outliers occur during the condition *uneven road* and result from the circumstance that the estimated RR is extremely low or high. Contrary, during the condition *engine on* the difference is lowest, compared to the other conditions, between estimated RR and reference. This indicates that the results are not always reliable and the method should be improved. These results could also be attributed to the poor signal quality and require improvements in signal reception.

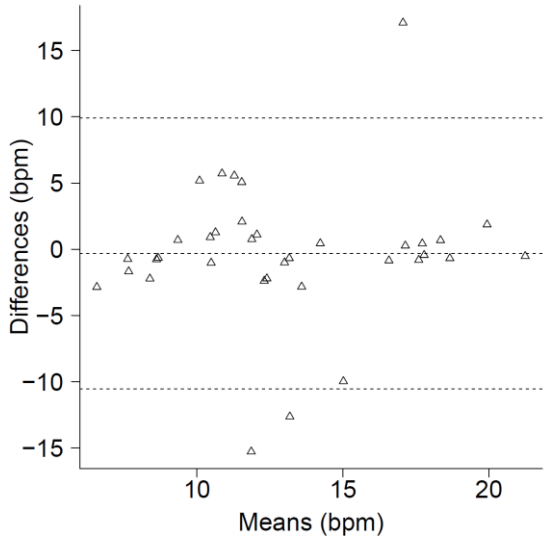

Figure 7. Bland-Altman plot of the difference between estimated RRs and reference RRs.

E. Comparison of Different Positions

The comparison indicates that the median for the placement at left and right side is significantly lower compared to front and back side. Additionally, the 25% and 75% quantiles of the placement of front and back side are larger than for the other.

TABLE I. DISTRIBUTION OF ESTIMATED RRS BY MEDIAN (Q2) AND THE 25% AND 75% QUANTILES (Q1, Q3) OF TWO WAYS OF IMU PLACEMENTS

IMU Position	Q1	Q2	Q3
L-R	0.70	0.93	1.72
F-B	0.72	2.15	2.85

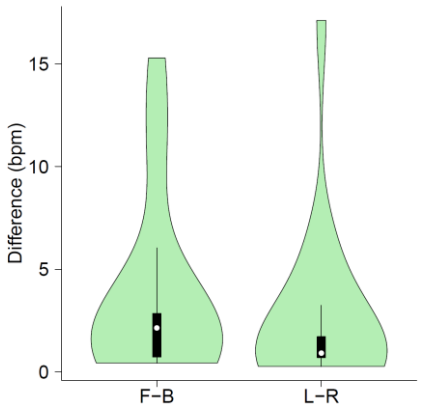

Figure 8. Violin plot of the difference between estimated RRs and the reference RRs for the two ways of IMU placements.

The distribution of the differences between estimated RRs and the reference RRs were visualized by the violin plot (Fig. 8). The wide green area indicates an intensive distribution to the difference values. When the IMU were attached to the L-R side of the car seat, the differences between estimated RRs and the reference RRs are lower in comparison to the placement of F-B side (Fig. 8). Therefore, towards recording noise information, the placement of the two IMU at the L-R side is better than placing at the F-B side.

F. Comparison of Different Conditions

Through comparison of the difference under the three driving conditions, the best results are achieved when *engine on* (Fig. 9). The noise is much higher on an *uneven road*. Therefore it becomes more difficult to measure respiration. In addition, the median for the condition uneven road is much higher.

TABLE II. DISTRIBUTION OF ESTIMATED RRS BY MEDIAN (Q2) AND THE 25% AND 75% QUANTILES (Q1, Q3) OF THREE DRIVING CONDITIONS.

Driving Condition	Q1	Q2	Q3
Engine on	0.62	0.81	1.25
Flat road	0.68	0.86	3.18
Uneven road	1.72	2.53	6.38

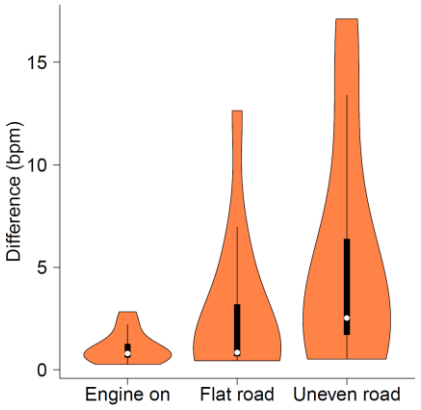

Figure 9. Violin plot of the difference between estimated RRs and the reference RRs for three driving conditions.

IV. Discussion

Noise is unavoidable for in-vehicle signal monitoring [6,7]. Because the recorded noise corresponds to the noise components in the respiratory signal, this work has exhibited the ability to leverage the information reflected by the additional IMU to suppress noise in the ECG unit data. However, for achieving more stable and reliable results, further efforts are still in need. The use of an additional sensor for noise reduction is also widely used for audio signals [11] and the results indicate that this approach is transferable to the recording of other vital signs in vehicles and contexts.

The results reveal that the estimated RR is sufficient. The placement of the additional IMU at the left and right sides of the seat is better than the front-back position. This finding could be a suggestion for the industry when a smart seat system is designed for vital sign measurement. Under the driving conditions *engine on* and *flat road,* the median of the difference between the estimated RR and reference RR amounts 0.81 bpm and 0.86 bpm. However, the median for the driving condition *uneven road* is 2.53 bpm. This can be explained by the fact that the noise component is clearly higher on an uneven road. If the smart seat system is to be used in a diversity of infrastructures, especially with low road quality, the reliability of the estimated RR should be improved by further approaches.

Other types of sensors might be also suitable to be integrated into the in-vehicle measurement. For instance, a camera attached to the windshield is able to monitor respiratory movements by detecting the changing color some specific areas of the face [13]. A strain sensor can be used to monitor the entire volume change of the upper body during inhalation and exhalation [14]. A measuring system with multiple sensors may improve the reliability by fusion the multiple estimated results, e.g., taking the mean of all estimated RR values from all applied sensors or by a majority vote. This creates information redundant systems, which measure the same signal in multiple ways, whereby this redundancy may increase the reliability. For increasing the safety, this approach of the decision in redundant systems is already applied to the development of autonomous vehicles [15,16]. Particularly, in severe weather conditions sensors as cameras show their limitations.

Ethical issues also require consideration due to vital signs monitoring. Because vital signs such as respiration allow conclusions about a person's health, thereby vital signs represent sensitive health data. In order to ensure the protection of this data, comprehensive security concepts must be implemented.

V. Conclusion

The results in this paper indicate that using additional accelerometers are an effective approach to reduce noise to estimate the RR during real driving. Appropriate positions for an additional accelerometer are the left and right side of the seat during autonomous driving. The paradigm shift in the automotive industry towards autonomous driving, where constant actions by a driver are no longer required, would enable the transformation of a vehicle into a diagnostic space. However, the problem of the high noise component during driving remains. To increase reliability, the demonstrated approach might be enhanced by an information redundant system.

Acknowledgment

We thank Dr. Axel Glanz from the Innovation Institute, Frankfurt, Germany, who provided the test vehicle. In addition, we thank all the testers, who voluntarily participated in the experiment and the independent persons, who established the ground truth for the respiration reference value.

References

[1] Brandrud AS, Schreiner A, Hjortdahl P, Helljesen GS, Nyen B, Nelson EC. Three success factors for continual improvement in healthcare: an analysis of the reports of improvement team members. BMJ Qual Saf. 2011 Mar;20(3):251-9.

[2] Thimbleby H. Technology and the future of healthcare. J Public Health Res. 2013 Dec 1;2(3):e28.

[3] Abraham C, Nishihara E, Akiyama M. Transforming healthcare with information technology in Japan: a review of policy, people, and progress. Int J Med Inform. 2011 Mar;80(3):157-70.

[4] Akhbardeh A, Junnila S, Koivuluoma M, Koivistoinen T, Varri A. The heart disease diagnosing system based on force sensitive chair's measurement, biorthogonal wavelets and neural networks. Proceedings of the 2005 IEEE/ASME International Conference on Advanced Intelligent Mechatronics; 2005 Jul 24-28; Monterey, CA. Piscataway: IEEE; 2005. p. 676-81.

[5] Herrmann A, Brenner W, Stadler R. Autonomous driving: how the driverless revolution will change the world. Bingley: Emerald Publishing Limited; 2018.

[6] Wusk G, Gabler H. Non-Invasive Detection of respiration and heart rate with a vehicle seat sensor. J Sensors. 2018 May;18(5):1463.

[7] Walter M, Eilebrecht B, Wartzek T, Leonhardt S. The smart car seat: personalized monitoring of vital signs in automotive applications. Pers Ubiquit Comput. 2011 Oct;15(7):707-15.

[8] Jafari Tadi M, Koivisto T, Pänkäälä M, Paasio A. Accelerometer-based method for extracting respiratory and cardiac gating information for dual gating during nuclear medicine imaging. Int J Biomed Imaging. 2014;2014:690124. Epub 2014 Jul 10.

[9] Drummond GB, Bates A, Mann J, Arvind DK. Validation of a new non-invasive automatic monitor of respiratory rate for postoperative subjects. Br J Anaesth. 2011 Sep;107(3):462-9.

[10] Wang J, Warnecke JM, Deserno TM. The vehicle as a diagnostic space: efficient placement of accelerometers for respiration monitoring during driving. Proceedings of the EFMI Special Topic Conference; 2019 Apr 7-10; Hannover, Germany. Amsterdam: IOS; 2019.

[11] Boll S. Suppression of acoustic noise in speech using spectral subtraction. IEEE Trans Signal Proc. 1979 Apr;27(2):113-20.

[12] Bernhard Lehnert. BlandAltmanLeh: Plots (Slightly Extended) Bland-Altman Plots. R package version 0.3.1 [software]. 2015 Dec 23 [cited 2019 Feb 4]. Available from: https://CRAN.Rproject.org/package=BlandAltmanLeh.

[13] Sato I, Nakajima M. Non-contact breath motion monitoring system in full automation. Proceedings of the 2005 IEEE Engineering in Medicine and Biology 27th Annual Conference; 2005 Jan 17-18; Shanghai, China. Piscataway: IEEE; 2006. p. 3448-51.

[14] Atalay O, Kennon WR, Demirok E. Weft-knitted strain sensor for monitoring respiratory rate and its electro-mechanical modeling. IEEE Sens J. 2015 Jan;15(1):110-22.

[15] Koopman P, Wagner M. Autonomous Vehicle Safety: An Interdisciplinary Challenge. IEEE Intell Transport Syst Mag. 2017 Jan 18;9(1):90-6.

[16] Wei J, Snider JM, Kim J, Dolan JM, Rajkumar R, Litkouhi B. Towards a viable autonomous driving research platform. Proceedings of the 2013 IEEE Intelligent Vehicles Symposium (IV); 2013 June 23-26; Gold Coast, Australia. Piscataway: IEEE; 2013. p. 763-70.